Single-Cycle Resonant Converters: A New Group of Quasi-Resonant Converters Suitable for High-Performance dc/dc and ac/ac Conversion Applications

Jung G. Cho and Gyu H. Cho, *Member, IEEE*

Abstract—**A new resonant switch and a new family of zero-current and zero-voltage mixed-mode switching quasi-resonant converters (QRC's) called single-cycle resonant converters (SCRC's) are proposed to improve the performance of the conventional QRC's. The proposed SCRC's, which include two active switches operated with zero-current switching (ZCS) and zero-voltage switching (ZVS), respectively, show very simple operation and easiness in control and analysis, and they overcome the limited load range characteristics of the conventional ZCS QRC's. Furthermore, the SCRC's can be applied even for a high-frequency ac chopper by replacing unidirectional switches with bidirectional ones. Steady-state operation and characteristics of the buck-type SCRC's are analyzed and compared with those of the buck-type full-wave QRC (FW-QRC). Experimental results at a 200-kHz, 1-kW level are shown to verify the operational principle and characteristics.**

I. Introduction

In switching power converters, the resonant conversion techniques have been renewed to replace the conventional PWM converters since their first introduction in the late 1960's. Thus far, a number of resonant converter topologies and control methods have been introduced, but most of them show complex topologies and/or difficulties in control, analysis, and design [1]–[4]. Furthermore, the ZCS or ZVS is often not satisfied, or the characteristics are substantially different from those of the well-known conventional PWM converters.

The quasi-resonant converters (QRC's) and the concept of the resonant switch were proposed by Liu *et al.* [5] and have been subject of intense research in recent years. They have well-known merits such as simple circuit topology, simple control and analysis, and similar dc characteristics to those of the PWM converters for full-wave mode operation. The topology of the resonant switch has also been extended and generalized, and several groups of QRC's have been suggested and experimentally verified at megahertz switching frequencies [6]–[9].

Even though the QRC's can be thought to be promising converters to replace the conventional PWM converters, they have several shortcomings that are unsolved as yet. In the case of half-wave mode operation, the QRC's show highly nonlinear and load-dependent characteristics, and thus, it is not easy to use them where the load variation is wide. On the other hand, for full-wave mode operation, the QRC's show the degrading efficiency characteristics according to decreasing load current from its maximum. Furthermore, in either case, the load range is limited by characteristic impedance of LC resonant elements to sustain ZCS operation and full control range.

In this paper, a new ZCS/ZVS resonant switch and a new family of ZCS/ZVS QRC's, known as single-cycle resonant converters (SCRC's), which improve the performance of the conventional QRC's and extend their applications to high-frequency ac choppers, are proposed. (Initial results of this work have been presented in [11].)

The proposed ZCS/ZVS resonant switch contains two active switches so that they can shape switching waveforms sinusoidally for a complete single resonant cycle, and therefore, ZCS and ZVS mixed-mode operation is always possible. This is the reason why the name of the converters made of the ZCS/ZVS resonant switch are known as SCRC's. The proposed SCRC's show similar characteristics to those of full-wave mode operated QRC's (FW-QRC's). The operation and analysis, however, are further simplified, and the limited-load range characteristic is overcome. In addition, the degrading efficiency characteristic at light-load range is improved. Furthermore, by replacing the switches with bidirectional ones, the SCRC's can also be used for the high-frequency ac chopper, which can be operated on four quadrants.

Circuit operating principle and steady-state analysis of the buck-type SCRC are described, and dc characteristics, switch stresses, and efficiency characteristic are also analyzed and compared with those of the FW-QRC's. Experimental results at the 200-kHz, 1-kW level are shown to verify the operational principle and characteristics.

Manuscript received July 12, 1990; revised January 23, 1991.

The authors are with the Department of Electrical Engineering, Korea Advanced Institute of Science and Technology, Seoul, Korea.

IEEE Log Number 9101046.

0278-0046/91/0800-0260$01.00 ©1991 IEEE

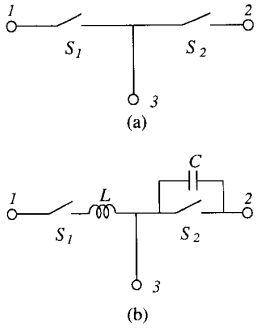

Fig. 1. (a) Three-terminal PWM switch; (b) general topology of three-terminal resonant switch.

II. Generation of ZCS/ZVS Resonant Switch

A general topology of three-terminal resonant switch is obtained by incorporating the LC resonant elements into the three-terminal PWM switch [10] shown in Fig. 1(a); an inductor is inserted in series with S_1 for zero current switching of S_1, and a capacitor is shunted to S_2 for zero voltage switching of S_2, as is shown in Fig. 1(b). According to the switch configurations, four resonant switches can be obtained: two are conventional ZCS resonant switches, and the other two are newly proposed ZCS/ZVS resonant switches as shown in Fig. 2. It is noted that the ZCS/ZVS resonant switches contain two active switches instead of one active and one passive switch configuration of the ZCS resonant switches. The operation of the proposed ZCS/ZVS resonant switches shows a quite different feature when compared with that of the ZCS resonant switches. Two switches are turned on and off alternately without any overlap or dwell period: S_1 is on for a complete resonant period, and S_2 is on during the rest of the switching period.

The buck-type SCRC's for dc/dc converter and ac chopper applications can be obtained from PWM buck converter by replacing the PWM switch with the ZCS/ZVS resonant switches, as is shown in Fig. 3. This approach can be extended to the other PWM dc/dc converters, and the corresponding types of SCRC's can be obtained.

III. Operation and Analysis of Buck-Type SCRC

A. Principle of Operation

Circuit topologies of the buck-type SCRC's are shown in Fig. 3(b) and (c) as a dc/dc converter and an ac chopper, respectively. To analyze their steady-state behavior, the following assumptions are made: All semiconductor switches and reactive elements are ideal, and L_f is much larger than L so that L_f, including the output side, is treated as a constant current source.

There are only two operating modes instead of four modes of the conventional QRC's, and the associated equivalent circuits for these modes are shown in Fig. 4. Suppose that the inductor current I_L and the capacitor voltage V_C are all initially zero, and S_2 carries the steady-state output current I_o. At time T_o, the switching cycle starts by turning on S_1 with zero current and turning off S_2 with zero voltage.

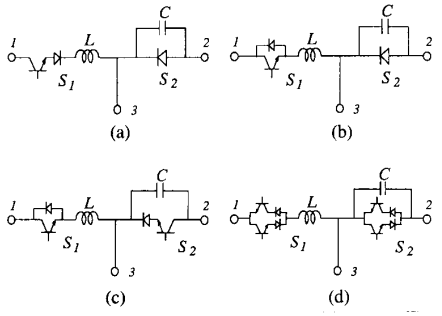

Fig. 2. Generation of resonant switches: (a) half-wave ZCS resonant switch; (b) full-wave ZCS resonant switch; (c) ZCS/ZVS resonant dc switch; (d) ZCS/ZVS resonant ac switch.

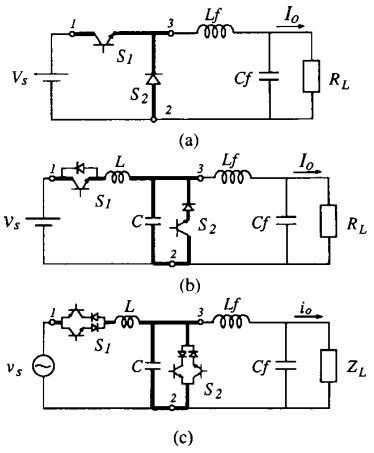

Fig. 3. Generation of the buck-type SCRC's from PWM buck converter: (a) PWM buck converter; (b) SCRC (dc/dc converter); (c) SCRC (ac chopper).

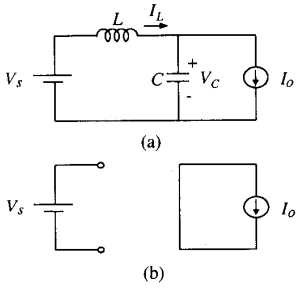

Fig. 4. Equivalent circuits for each switching mode: (a) resonant mode; (b) freewheeling mode.

1) Resonant Mode (T_o, T_r): As shown in Fig. 4(a), the voltage source V_s and the current source I_o are simultaneously applied to LC resonant circuit at time T_o in series and parallel, respectively. Consequently, the resonant circuit is excited by two step inputs. The state equations are given by

$$L\frac{dI_L(t)}{dt} = V_s - V_C(t) \tag{1a}$$

$$C\frac{dV_C(t)}{dt} = I_L(t) - I_o \tag{1b}$$

with the initial conditions $I_L(0) = 0$, $V_C(0) = 0$. Thus, I_L and V_C become

$$I_L(t) = \sqrt{(V_s/Z_r)^2 + I_0^2} \cdot \sin\left(\omega t - \tan^{-1}(Z_r I_o / V_s)\right) + I_o \quad (2a)$$

$$V_C(t) = \sqrt{(Z_r I_o)^2 + V_s^2} \cdot \sin\left(\omega t - \tan^{-1}(V_s / Z_r I_o)\right) + V_s \quad (2b)$$

where $Z_r = \sqrt{L/C}$, $\omega_r = 1/\sqrt{LC}$, $T_r = 1/f_r = 2\pi/\omega_r$. The resonant inductor current and capacitor voltage show all sinusoidal waveforms with dc offset I_o and V_s, respectively, and it should be noted that the amplitudes of resonant current and voltage are varied according to the load current I_o instead of fixed values of the conventional QRC's. At time Tr, after one complete resonant period, they return to the initial states of this mode: $I_L(T_r) = 0$, $V_C(T_r) = 0$.

2) Freewheeling Mode (T_r, T_s): At time T_r, S_1 is turned off with zero current, and S_2 is turned on with zero voltage simultaneously, as shown in Fig. 4(b), and then, the output current freewheels through the S_2 until T_s, which is the end of switching cycle:

$$I_L(t) = 0 \quad (3a)$$

$$V_C(t) = 0. \quad (3b)$$

Overall switching waveforms are shown in Fig. 5.

B. State Plane Analysis

To provide more comprehensive analysis, the switching behavior of the buck-type SCRC can be described on the state plane. From (2) and (3), a steady-state trajectory in a normalized state plane $I_{LN} - V_{CN}$ is obtained, as is shown in Fig. 6, where V_s/Z_r and V_s are the normalization factors for current and voltage, respectively. For the resonant mode, the state trajectory is represented by a circle with its center located at $(1, I_{ON})$ and radius R as follows:

$$(I_{LN} - I_{ON})^2 + (V_{CN} - 1)^2 = R^2 \quad (4)$$

where the R is given as

$$R = \sqrt{\frac{(Z_r I_o)^2 + V_s^2}{V_s^2}} \geq 1. \quad (5)$$

For the freewheeling mode, the state trajectory simply stays at the origin. Fig. 7 shows the variations of the trajectory according to load current. From Figs. 6 and 7, it can be seen that the state trajectory of the SCRC consists of only two segments, corresponding to two modes of operation, and the radius of circle trajectory is varied according to load current, which is comparable to four segments of trajectory and the fixed radius of the ZCS-QRC [6]. Furthermore, there are no unfamiliar trajectories [6], even though the switching frequency is increased to close to resonant frequency.

C. Operation for ac Chopper Application

To illustrate the operation of the buck-type SCRC as an ac chopper shown in Fig. 3(c), the combination of output filter

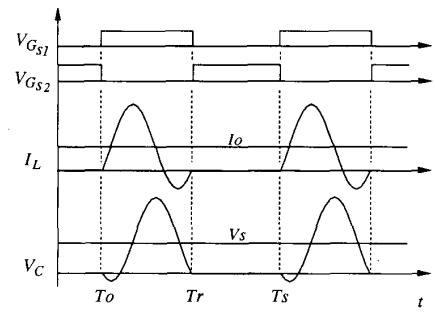

Fig. 5. Operational waveforms of the buck-type SCRC.

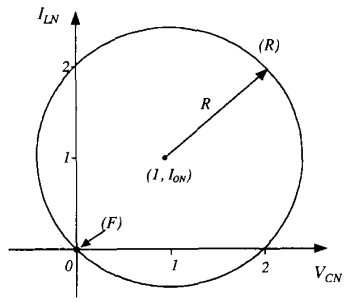

Fig. 6. State plane trajectory of the buck-type SCRC.

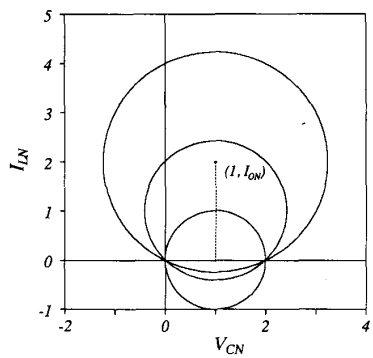

Fig. 7. Variation of the trajectory according to load current (dotted line: $V_{SN} - I_{ON}$ trajectory).

$L_f C_f$ and load is still treated as a constant current source. Since the switching frequency is generally much higher than the input frequency, the input voltage v_s and the output current i_o can be treated as constant values during a switching period. Thus, the microscopic operation is the same as that of the dc/dc converter.

Fig. 8 shows macroscopic waveforms of the buck-type SCRC ac chopper. To reveal the switching operation clearly, the switching frequency is chosen to be seven times the input frequency. The resonant current, voltage waveforms and state plane trajectories are shown in Figs. 8 and 9 for resistive and inductive load, respectively. The amplitude of the output voltage can be controlled by the ratio of the switching frequency and resonant frequency for any kind of load since it has four-quadrant operation capability.

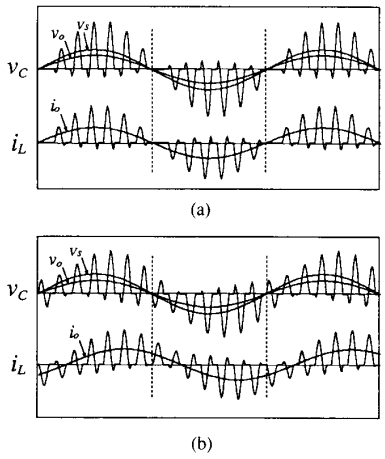

Fig. 8. Illustrative waveforms of the SCRC for ac chopper application: (a) resistive load case; (b) inductive load case.

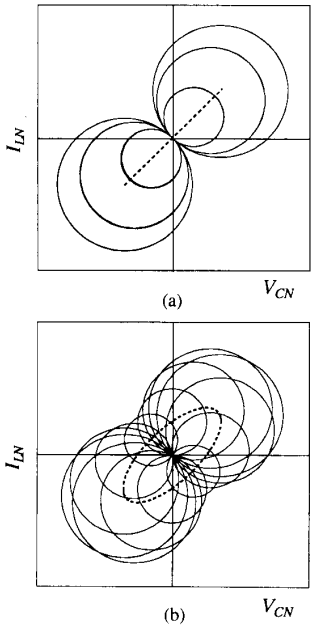

Fig. 9. State plane trajectories for ac chopper application: (a) resistive load case; (b) inductive load case (dotted line: $V_{SN} - I_{ON}$ trajectory).

IV. Characteristics

A. dc Voltage Conversion Ratio of the Buck-Type SCRC

The output voltage V_o of the buck-type SCRC can be solved by equating the input energy per cycle E_i to the output energy per cycle E_o where

$$E_i = V_s \cdot \int_{T_o}^{T_s} I_L(t)\,dt = V_s \cdot \int_{T_o}^{T_r} I_L(t)\,dt \tag{6}$$

$$E_o = V_o I_o T_s. \tag{7}$$

From (6) and (7), we obtain

$$V_o = \frac{T_r}{T_s} V_s = \frac{f_s}{f_r} V_s. \tag{8}$$

This relationship shows that the dc voltage conversion ratio of the buck-type SCRC depends linearly on the normalized switching frequency f_s/f_r, and it is plotted in Fig. 10 with that of the FW-QRC for comparison. The voltage conversion ratios of the buck-type QRC are well known; they show nonlinear and load-dependent characteristics for half-wave mode operation while linear and almost load-independent characteristics for full-wave mode operation. In either case, however, the load ranges are limited by Z_r for unlimited control range, or the control ranges are limited by R/Z_r for unlimited load range. Fig. 10(a) shows that the control range of the FW-QRC is limited by R/Z_r for unlimited load range. The voltage conversion ratio of the proposed buck-type SCRC, however, shows linear and completely load-independent characteristics like that of the PWM buck converter. Thus, it overcomes the limited load or control range characteristics of the QRC's, as is shown in Fig. 10(b).

DC voltage conversion ratios of the other types of SCRC's can easily be derived, and their characteristics are the same as those of the corresponding PWM converters as well.

B. Switch Stresses of the Buck-Type SCRC

The peak voltage stress of S_1 and the peak current stress of S_2 are sustained with V_s and I_o, respectively, as are those of the FW-QRC. The peak current stress of S_1 and the peak voltage stress of S_2 are affected directly by the resonant current I_L and voltage V_C, respectively. Fig. 11 shows the variations of resonant current and voltage waveforms according to load current for FW-QRC and SCRC, and it is seen that the peak resonant current and voltage of SCRC is varied according to load current in contrast with fixed ones of the FW-QRC. From (2) and [5], the peak current stresses of S_1 and voltage stresses of S_2 for the FW-QRC and SCRC can easily be derived. The peak current stresses of S_1 are obtained as follows:

$$I_{S_1,\text{FW-QRC}} = \frac{V_s}{Z_r} + I_o. \tag{9}$$

$$I_{S_1,\text{SCRC}} = \sqrt{\left[\frac{V_s}{Z_r}\right]^2 + I_o^2} + I_o. \tag{10}$$

The normalized peak current stresses for the FW-QRC and SCRC according to the normalized load current with parameter Z_r are shown in Fig. 12(a) and (b), respectively. It can be seen that the peak current stresses are decreased by increasing the characteristic impedance Z_r in either case. Therefore, it is required that Z_r should be increased as high as possible to reduce the peak current stress of S_1. The Z_r of the FW-QRC, however, is limited by $Z_{r\,\max}$,

$$Z_{r\,\max} = \frac{V_s}{I_{o\,\max}} \tag{11}$$

whereas Z_r of the SCRC is unlimited. Thus, the peak current

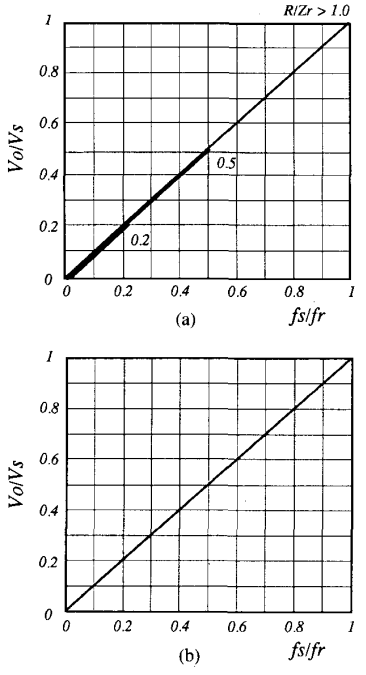

Fig. 10. DC voltage conversion ratio characteristics of the buck-type QRC's: (a) conventional FW-QRC; (b) SCRC.

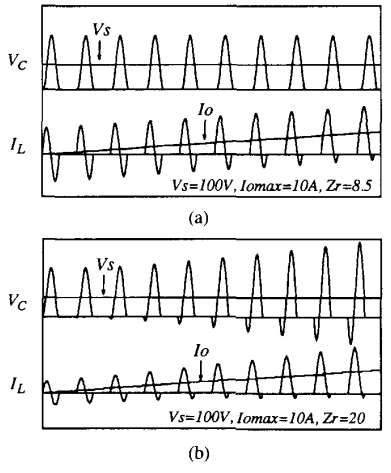

Fig. 11. Comparisons of the resonant currents and voltages waveforms with load current variation: (a) FW-QRC; (b) SCRC.

stress of the SCRC at low load current can be reduced to be much smaller than that of the FW-QRC, and this fact is clearly revealed in Fig. 11.

Similarly, the peak voltage stresses of S_2 are obtained as follows:

$$V_{D_2,\text{FW-QRC}} = 2V_s \tag{12}$$

$$V_{S_2,\text{SCRC}} = \sqrt{(Z_r I_o)^2 + V_s^2} - V_s \tag{13a}$$

$$V_{D_2,\text{SCRC}} = \sqrt{(Z_r I_o)^2 + V_s^2} + V_s \tag{13b}$$

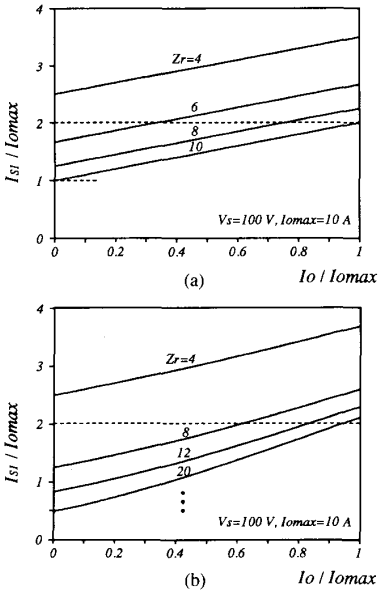

Fig. 12. Comparison of the peak current stress characteristics of $S1$: (a) FW-QRC; (b) SCRC.

The peak voltage stress of $S_2(=D_2)$ for the FW-QRC is fixed to $2V_s$ since the peak resonant voltage V_C is fixed. In the case of SCRC, however, the peak voltage stress of S_2 is varied since the peak resonant voltage V_C is varied according to load current. The positive part of V_C is blocked by the reverse blocking diode D_2, and only the negative part of V_C is applied to the active switch S_2, as is shown in (13a) and (13b). For ac chopper application of the SCRC, however, either polarity of V_C is implied to the active device S_2. The normalized peak voltage stresses of S_2 and D_2 according to the normalized load current are plotted with the parameter Z_r, in Fig. 13(a) and (b), respectively. It can be seen that the peak voltage stresses of S_2 and D_2 are increased directly by increasing Z_r.

In designing the SCRC's, therefore, the peak current stress of S_1 and the peak voltage stress of S_1 should be compromised by moderate selection of Z_r.

C. Efficiency Comparison

To show the improvement of the degrading efficiency characteristic, the overall efficiencies of the FW-QRC and SCRC are evaluated and compared. The lossy components are modeled as shown in Fig. 14 to evaluated conduction losses. The switching loss, LC filter loss, and the other losses of two converters are quite similar and ignored here to focus the point of interest on efficiency comparison. Efficiencies according to load current are obtained by computer simulation with the following parameters:

$$R_{DS,S_1} = 0.085\ \Omega(\text{IRF250}), \qquad R_L = 30\ \text{m}\Omega,$$

$$R_{DS,S_2} = 0.055\ \Omega(\text{IRF150}), \qquad V_D = 0.9\ \text{V}.$$

The characteristic impedance of the FW-QRC is chosen in 8.5 Ω, which is obtained from the maximum characteristic

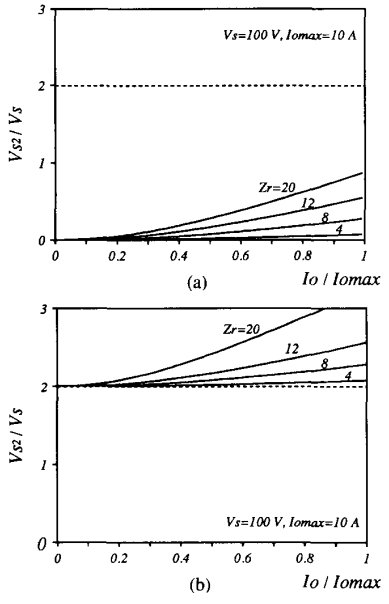

Fig. 13. Peak voltage stress characteristics of $S2$: (a) active switch (S_2); (b) reverse blocking diode (D_2) or switch (S_2) in the case of ac chopper application.

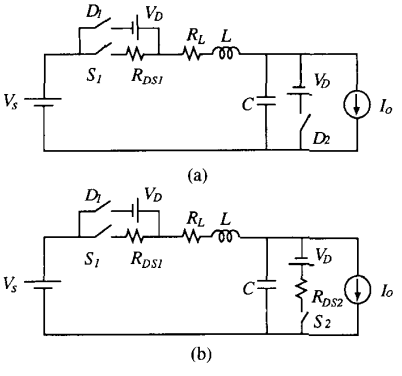

Fig. 14. Simple models for evaluation of efficiencies: (a) FW-QRC; (b) SCRC.

impedance $Z_{r\,\max}(= 10\ \Omega)$ with a margin for assuring a ZCS of S_1. Since Z_r of the SCRC, however, is unlimited, it is chosen here as 16 Ω as an example. Fig. 15 shows the comparison of the efficiencies according to load current, and it can be seen that the efficiency of the SCRC at low-load current is considerably higher than that of the FW-QRC.

V. Experimental Results

The 1-kW-level buck-type SCRC's for dc/dc converter and ac chopper are constructed and tested to verify the operational principle and characteristics. The circuit diagrams in either application are shown in Fig. 16(a) and (b), respectively, with the component values. The resonant frequency and the characteristic impedance of LC resonant circuit are chosen as 200 kHz and 16 Ω, respectively.

The experimental waveforms of dc/dc converter application are shown in Fig. 17 with good agreement with theories.

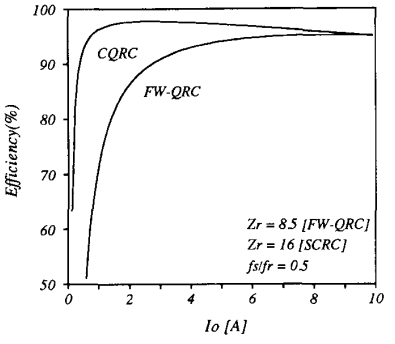

Fig. 15. Efficiency characteristics of FW-QRC and SCRC.

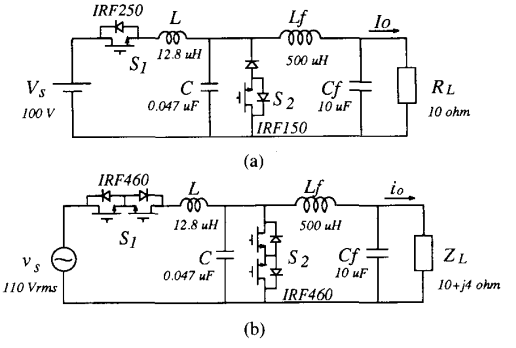

Fig. 16. Circuit diagrams of the buck-type SCRC's for experiment: (a) dc/dc converter application; (b) ac chopper application.

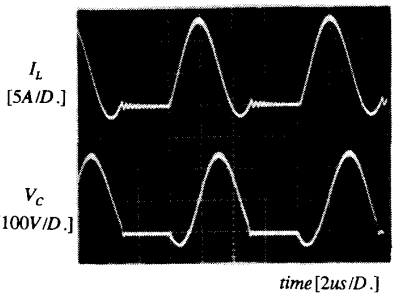

Fig. 17. Operational waveforms of the buck-type SCRC for dc/dc converter: fr = 200 kHz, fs = 120 kHz.

Fig. 18 shows the voltage conversion ratios, and it can be seen that the control range is unlimited even though the $R/Zr \leq 1$. The small discrepancy from the theoretical values is mainly caused by conduction loss. Fig. 19 shows the measured efficiencies for FW-QRC and SCRC. It can be seen that the degrading efficiency characteristic of FW-QRC is improved in the SCRC. The measured values, however, show lower than the calculated ones in Section IV-C, which is caused by unconsidered losses. Figs. 20 and 21 show the resonant and input/output waveforms of the ac chopper application of the SCRC with resistive load (10 Ω) and inductive load ($10 + j4$ Ω), respectively. The amplitude of the output voltage can be controlled by varying the normalized switching frequency f_s/f_r for any kind of load, and

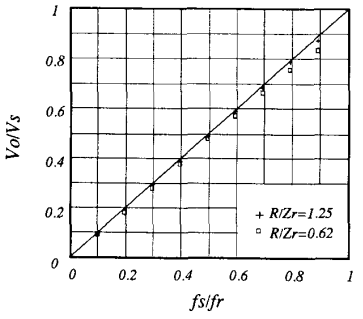

Fig. 18. Measured voltage conversion ratios of the buck-type SCRC.

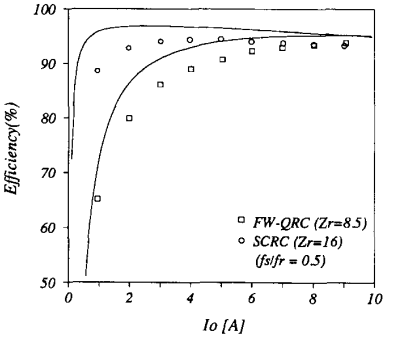

Fig. 19. Measured efficiencies of FW-QRC and SCRC.

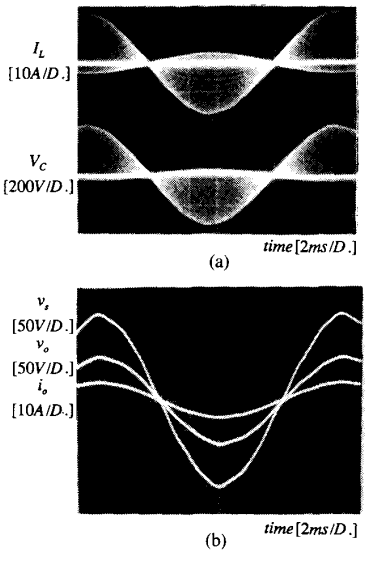

Fig. 20. Experimental waveforms of the buck-type SCRC for ac chopper application with resistive load ($V_o = 0.5\ V_s$, $R = 10\ \Omega$): (a) resonant current and voltage waveforms; (b) input and output waveforms.

thus, it can be seen that the SCRC has four quadrant operation capability.

VI. Conclusion

A new ZCS/ZVS resonant switch and a new family of ZCS/ZVS QRC's, known as single-cycle resonant converters (SCRC's) are presented. The steady-state operation, analysis, and several characteristics of the proposed SCRC's are analyzed and verified experimentally at 200-kHz and 1-kW levels, and most of the characteristics are compared with those of the FW-QRC's.

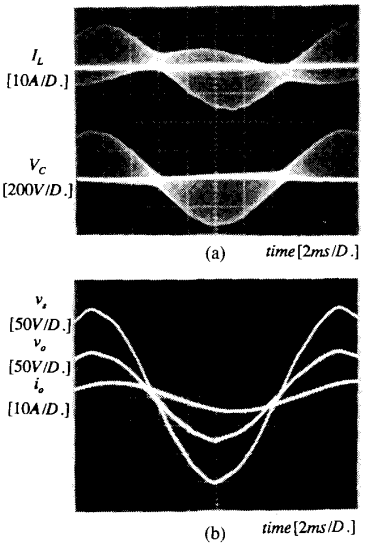

Fig. 21. Experimental waveforms of the buck-type SCRC for ac chopper application with inductive load ($V_o = 0.5\ V_s$, $Z_L = 10 + j4\ \Omega$): (a) resonant current and voltage waveforms; (b) input and output waveforms.

It is shown that the proposed SCRC's operate with ZCS and ZVS mixed mode and have very similar characteristics as those of the PWM converters with frequency control rather than duty ratio control. In addition, the proposed SCRC's have several other distinctive advantages over the conventional ZCS-QRC's, such as the following:

1) Simple operation
2) easy analysis and control
3) unlimited load range
4) improved efficiency (compared with FW-QRC's).

Furthermore, by using the bidirectional switches, the proposed SCRC's can be used for the high-performance ac choppers as well.

References

[1] R. L. Steigerward, "High frequency resonant transistor dc-dc converters," *IEEE Trans. Ind. Electron.*, vol. IE-31, no. 2, pp. 181-192, May 1984.

[2] V. Vorperian and S. Cuk, "A complete dc analysis of the series resonant converter," in *IEEE PESC Rec.*, 1982, pp. 85-100.

[3] I. J. Pitel, "Phase-modulated resonant power conversion techniques for high frequency link inverters," *IEEE Trans. Industry Applications*, vol. IA-22, no. 6, pp. 1044-1051, Nov/Dec. 1986.

[4] V. Vorperian, "Quasi-square-wave converters Topologies and analysis," *IEEE Trans. Power Electron.*, vol. 3, no. 2, pp. 183-191, Apr. 1988.

[5] K. H. Liu, R. Oruganti, and F. C. Lee, "Quasi-resonant converter—Topologies and characteristics," *IEEE Trans. Power Electron.*, vol. PE-2, no. 1, pp. 62-71, Jan. 1987.

[6] M. M. Jovanovic, K. H. Liu, R. Oruganti, and F. C. Lee, "State-plane analysis of quasi-resonant converters," *IEEE Trans. Power Electron.*, vol. PE-2, no. 1, pp. 36-44, Jan. 1987.

[7] T. Zeng, D. Y. Chen, and F. C. Lee, "Variations of quasi-resonant dc-dc converter topologies," in *IEEE PESC Rec.*, 1986, pp. 381-392.

[8] K. D. T. Ngo, "Generalization of resonant switches and quasi-resonant dc-dc converters," in *IEEE PESC Rec.*, 1987, pp. 395-403.
[9] W. A. Tabisz and F. C. Lee, "Zero-voltage-switching multi-resonant technique—A novel approach to improve performance of high-frequency quasi-resonant converters," in *IEEE PESC Rec.*, Apr. 1988, pp. 9-17.
[10] R. Tymerski, V. Vorperian, F. C. Lee, and W. Baumann, "Nonlinear modeling of the PWM switch," *IEEE Trans. Power Electron.*, vol. 4, no. 2, Apr. 1989.
[11] J. G. Cho and G. H. Cho, "Single cycle resonant converters: a new family of resonant converters," in *Proc. Int. Symp. Power Electron.*, May 1989, pp. 259-266.